Interactions of Hydrophobin Proteins in Solution Studied by Small-Angle X-Ray Scattering

Kaisa Kisko,* Géza R. Szilvay,† Ulla Vainio,* Markus B. Linder,† and Ritva Serimaa*
*Department of Physical Sciences, University of Helsinki, FI-00014 HU, Finland; and †VTT, Technical Research Centre of Finland, FI-02044 VTT, Finland

ABSTRACT Hydrophobins are a group of very surface-active, fungal proteins known to self-assemble on various hydrophobic/hydrophilic interfaces. The self-assembled films coat fungal structures and mediate their attachment to surfaces. Hydrophobins are also soluble in water. Here, the association of hydrophobins HFBI and HFBII from *Trichoderma reesei* in aqueous solution was studied using small-angle x-ray scattering. Both HFBI and HFBII exist mainly as tetramers in solution in the concentration range 0.5–10 mg/ml. The assemblies of HFBII dissociate more easily than those of HFBI, which can tolerate changes of pH from 3 to 9 and temperatures in the range 5°C–60°C. The self-association of HFBI and HFBII is mainly driven by the hydrophobic effect, and addition of salts along the Hofmeister series promotes the formation of larger assemblies, whereas ethanol breaks the tetramers into monomers. The possibility that the oligomers in solution form the building blocks of the self-assembled film at the air/water interface is discussed.

INTRODUCTION

Hydrophobins are a group of very surface-active proteins (1). They are small (~10 kDa) proteins that originate from filamentous fungi, where they coat the spores and aerial structures (2), mediate the attachment of fungal structures to hydrophobic surfaces (3), and affect the cell wall composition (4). Hydrophobins self-assemble at the air/water interface and lower the surface tension of water (5). Furthermore, they have been shown to also self-assemble at interfaces between oil and water (3,6) and water and a hydrophobic solid (3).

The primary structure of hydrophobins is characterized by a conserved pattern of eight cysteine residues. These form four intramolecular disulfide bridges. Hydrophobins are further divided into classes I and II based on their hydropathy patterns (7), although the amino acid sequence similarity both within and between the classes is small. However, in all the published atomic resolution structures (8–10), the folds of the monomers are similar. One side of the monomer surface contains only aliphatic side chains, creating a hydrophobic patch to the otherwise fairly hydrophilic surface.

Hydrophobins are very soluble in water up to concentrations of at least 100 mg/ml (1). In solution hydrophobins associate into oligomers in a concentration-dependent manner. At low concentrations on the order of a few μg/ml, hydrophobins exist primarily as monomers (11,12). As the concentration is increased, hydrophobins form oligomers. According to various light scattering techniques, the class I hydrophobin SC3 from *Schizophyllum commune* mainly forms dimers around 1 mg/ml (11), whereas small-angle x-ray scattering (SAXS) has shown that the class II *Trichoderma reesei* hydrophobins HFBI and HFBII exist as tetramers at 10 mg/ml (13). The association in solution and the self-assembly at the air/water interface have both been attributed to the amphiphilic structure of the hydrophobin monomer (8), but their exact relationship is still unclear. On one hand, for class II hydrophobins a surfactant-like behavior due to the amphiphilic monomer has been suggested (12). On the other hand, for class I hydrophobins the association in solution has been seen as a first step toward self-assembly on the air/water interface (11).

In this work we investigated the self-association of hydrophobins in solution in more detail. The hydrophobins chosen for this study are the well-characterized class II *T. reesei* hydrophobins HFBI (14) and HFBII (15) with 75 and 71 amino acids, respectively. They have been studied as thick coatings (16) and Langmuir-Blodgett mono- (17,18) and multilayers (19) on solid substrates. In most cases HFBI and HFBII form similar, hexagonally ordered films. HFBI and HFBII have also been grown as single crystals, where the asymmetric, repeating units of HFBI (Protein Data Bank entry 2FZ6) (9) and HFBII (Protein Data Bank entry 1R2M) (8) are a tetramer and a dimer with radii of gyrations (Rgs) of 21.1 Å and 18.0 Å, respectively (Table 1).

Here we present a systematic SAXS study of the association of HFBI and HFBII in solution. SAXS is a versatile tool for studies of the size and shape of macromolecules in solution and their interactions. At low protein concentrations, the macromolecules can be considered independent of each other and their size and shape can be probed (20). At higher concentrations the interactions between the macromolecules or their aggregates can be studied (21,22). The hydrophobin solution experiments are conducted in the concentration range where hydrophobins form oligomers, but interactions between the oligomers can be regarded as negligible. The experiments at different analyte concentrations, temperatures,

Submitted May 9, 2007, and accepted for publication August 15, 2007.

Address reprint requests to Kaisa Kisko, University of Helsinki, Dept. of Physical Sciences, PO Box 64, Gustaf Hällströmin katu 2, Helsinki 00014 HU, Finland. Tel.: 358-09-19150628; E-mail: kaisa.kisko@helsinki.fi.

Editor: Jill Trewhella.

0006-3495/08/01/198/09 $2.00

doi: 10.1529/biophysj.107.112359

TABLE 1 The radius of gyration (Rg) and molecular mass (MM) of different HFBI and HFBII oligomers calculated from the crystal structures 2FZ6 and 1R2M, respectively

	HFBI		HFBII	
Oligomer	Rg (Å)	MM (kDa)	Rg (Å)	MM (kDa)
Monomer	14.0	7.5	11.8	7.2
Dimer	17.8	15.1	18.0	14.4
Tetramer	21.1	30.1	20.7	28.8

2FZ6 data from Hakanpää et al. (9); 1R2M data from Hakanpää et al. (8).

and pH provide information on the structure of the protein assemblies in response to changes in the conditions. Fungi secrete hydrophobins into the aqueous culture medium (5), where the hydrophobins are exposed to variations, for example, in temperature and pH. Moreover, the SAXS measurements can be used to probe the nature of the intermolecular interactions. Understanding these interactions provides a key to understanding the function of the proteins and their roles in the fungal life.

MATERIALS AND METHODS

Protein purification and sample preparation

The proteins HFBI and HFBII were produced and purified as described previously (17). In the SAXS measurements all the solutions contained 50 mM sodium acetate buffer at pH 5, unless otherwise stated. The protein solutions were briefly treated in an ultrasonicator water bath and placed into a 100 μl sample cell with flat polystyrene windows for the measurements. Before and after each sample, scattering from the corresponding buffer solution was measured and the sample cell was thoroughly washed with ethanol and 3% HCl and then dried. To prevent radiation damage 2 mM dithiothreitol (DTT) was added to all the solutions just before the measurement. At pH 5, this does not cause unfolding of the proteins, because higher DTT concentrations and high temperatures are required for the reduction of the internal disulfide bonds of HFBI and HFBII (12). The reactivity of DTT is highest above pH 7.

HFBI and HFBII were studied as a function of concentration at 0.5, 1, 2.5, 5, and 10 mg/ml. The concentration 2.5 mg/ml was used in the rest of the measurements. HFBI and HFBII were measured in 50 mM glycine at pH 3, 50 mM sodium acetate at pH 4 and at pH 5, 50 mM sodium phosphate at pH 6, 50 mM sodium phosphate at pH 7, 50 mM Hepes at pH 7, and 50 mM Tris-HCl at pH 9, and at temperatures 6°C, 11°C, 16°C, 20°C, 40°C, and 60°C in 50 mM sodium acetate at pH 5, using a fresh sample at each temperature. The effects of solvent were studied in 25%, 50%, and 65% ethanol solutions. The impact of salts was exemplified with 0.5 M NaCl, $(NH_4)_2SO_4$, and $MnSO_4$ in 50 mM sodium acetate at pH 5.

SAXS measurements and data analysis

The experiments were conducted at the beamline X33 at EMBL/DESY, Hamburg. The wavelength was $\lambda = 1.5$ Å. The angular scale was calibrated using a Silver Behenate standard sample and was $0.01\ 1/\text{Å} < q < 0.5\ 1/\text{Å}$. Here the length of the scattering vector is defined as $q = 4\pi\sin\theta/\lambda$, where 2θ is the scattering angle. The intensity was recorded with a Mar345 image plate detector. The measurement times varied from 60 s for the higher concentrations to 2×120 s for the lower ones. A solution of bovine serum albumin (BSA) ($c = 4.01$ mg/ml, molecular mass (MM) 66 kDa) was measured for calibration of intensity at zero angle $I(q = 0)$.

The preliminary data treatment (masking, integration, correction for detector response) was done using the software at the beamline. The data analysis was made with the program package ATSAS (23). The backgrounds from the buffers were subtracted with PRIMUS. The distance distribution functions of the proteins were calculated using GNOM. The GNOM runs were given as an input for the ab initio bead modeling program DAMMIN or the ab initio protein-chain compatible modeling program GASBOR. The results were compared to the scattering curves of the oligomers in the single crystals (8,9) calculated using CRYSOL. The experimental scattering curves were also fitted using SASREF, with the structure of the oligomer in the single crystal as a starting point. In this approach the monomers are moved with respect to each other to find the best fit to the experimental intensity. Finally, the possible presence of multiple aggregation states in solution was studied using the program OLIGOMER, which fits the volume fractions of oligomers with known scattering patterns.

RESULTS

HFBI and HFBII in aqueous solution as a function of concentration

The scattering curves of HFBI as a function of concentration are shown in Fig. 1 *A*. The overall shape of the curves is similar, and the main features can be seen even in the lowest concentration, $c = 0.5$ mg/ml. This suggests that the size and shape of the protein assemblies are the same at all concentrations. The slight upturn in the intensity for the 0.5 mg/ml solution at low q can indicate the presence of a small number of larger oligomers. However, we cannot exclude the possibility that the upturn arises from incomplete background subtraction. The data from samples such as this were analyzed using only a restricted q-range, starting from 0.025 or 0.035 1/Å, as in Verheul et al. (24).

Table 2 shows, as a function of protein concentration, the Rg and the MM of HFBI. The Rg has been calculated using the Guinier approximation. The MMs have been calculated from the extrapolated $I(q = 0)$ values (25) using the BSA standard. At the lowest concentration the MMs correspond to a tetramer (Table 1), but the Rg is larger than that of the single crystal tetramer. The Rg of HFBI increases with concentration from 0.5 to 5 mg/ml but decreases slightly from 5 to 10 mg/ml. A similar behavior is noted in $I(0)$. Two different reasons can contribute to these changes: First, assuming there is a mixture of different oligomers in the solution, the increase in Rg from 0.5 mg/ml to 5 mg/ml can result from a shift toward larger oligomers. Second, the decrease of Rg and $I(0)$ above 5 mg/ml can be attributed to the rise of repulsive interactions between the oligomers (21).

The distance distribution functions [$p(r)$-functions] of HFBI at different concentrations (Fig. 2) indicate that there is no major change in the aggregation state of the proteins. The $p(r)$-functions have the same shape and resemble each other very closely. The only differences are in the largest diameters of the particles: they behave in a way similar to the Rg, grow until 5 mg/ml, and then decrease. It indicates that the shape of the dominant protein assembly remains the same, but the proportion of larger oligomers in solution increases.

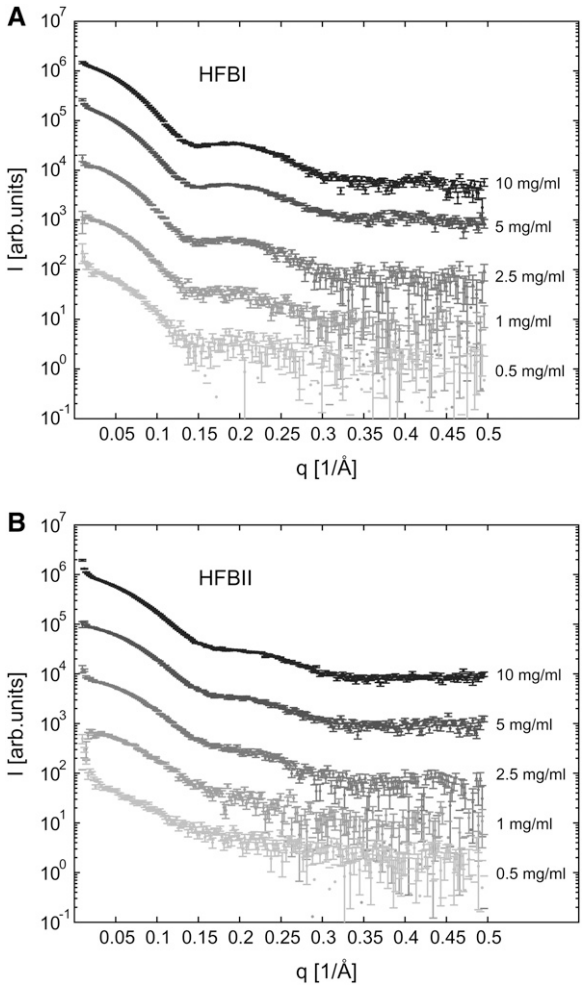

FIGURE 1 The SAXS intensities of (*A*) HFBI and (*B*) HFBII as a function of concentration, the highest concentration at the top. The intensities have been divided by the concentration and vertically lifted with respect to each other, all by a decade compared to the previous one. Only every 10th point is shown for clarity.

The shape of the HFBI assemblies in solution was modeled using the data at 1 mg/ml to minimize the proportion of the larger assemblies. Fig. 3 *A* shows the experimental intensity of HFBI at 1 mg/ml, the scattering intensity of the tetramer in the single crystal calculated by CRYSOL, and the intensities fitted with SASREF and DAMMIN. Fig. 3 *B* shows the corresponding models. Comparison of the single crystal structure and DAMMIN model confirms that HFBI forms tetramers at 1 mg/ml. The shape of the tetrameric assembly is more elongated in the aqueous solution than in the single crystal. The calculated Rg of the model tetramer based on the crystal structure (Fig. 3 *B*) is 21.1 Å, whereas the experimental Rg is considerably larger, 25.1 Å.

The behavior of HFBII as a function of concentration is very similar to that of HFBI, except that the radii of gyrations are smaller (Table 2). The shapes of the scattering curves (Fig. 1 *B*) do not change as a function of concentration, except for the data at 0.5 mg/ml, which have lost most of the features at

TABLE 2 The experimental Rg and MM

	HFBI		HFBII	
	Rg (Å)	MM (kDa)	Rg (Å)	MM (kDa)
c (mg/ml)				
0.5	24.8 ± 1.0	28	20.2 ± 1.0	16
1.0	25.1 ± 0.2	30	20.1 ± 0.2	19
2.5	26.2 ± 0.4	37	21.3 ± 0.2	22
5.0	28.0 ± 1.4	50	22.0 ± 0.3	25
10.0	27.2 ± 0.9	36	23.2 ± 0.8	25
T (°C)				
6	26.0 ± 0.2	35	20.9 ± 0.2	20
11	26.6 ± 0.8	35	21.0 ± 0.1	20
16	25.8 ± 0.2	35	20.7 ± 0.2	22
20	26.1 ± 0.4	30	21.3 ± 0.1	20
40	24.5 ± 0.3	30	22.1 ± 0.4	27
60	24.5 ± 0.2	38	21.8 ± 0.2	30
pH				
3	25.8 ± 0.4	32	–	–
4	25.7 ± 0.2	35	20.9 ± 0.1	20
5	26.2 ± 0.4	37	21.3 ± 0.2	22
6	26.2 ± 0.8	34	21.4 ± 0.5	23
7 (Hepes)	24.3 ± 0.1	25	21.3 ± 0.2	19
7 (NaP)	–	–	21.6 ± 0.3	19
9	23.2 ± 0.5	19	20.4 ± 0.2	13

The error estimates for the Rg values are obtained from the differences between the GNOM values and the direct fit to the Guinier law.
A missing value indicates a nonlinear Guinier regime. The error estimates for the MMs are 15%–20%, mainly due to the uncertainties in the concentrations and electron densities (24,25,30).

larger angles. As in the case of HFBI, the upturn in intensity at 0.5 mg/ml at the smallest angles arises either from larger aggregates or incomplete background subtraction. This part of the intensity curve was again excluded from the data analysis. The Rg and $I(0)$ of HFBII grow as a function of concentration (Table 2). The MM at the lowest concentration, 0.5 mg/ml, is close to that of a dimer but shifts toward the tetramer mass above 1 mg/ml. The experimental Rg at 0.5 mg/ml is 20.1 Å; the calculated Rg of the dimer in the HFBII crystal (8) is 18.0

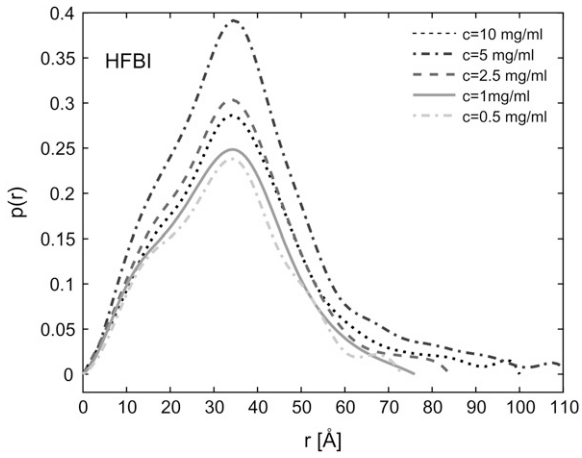

FIGURE 2 The distance distribution functions of HFBI at different concentrations.

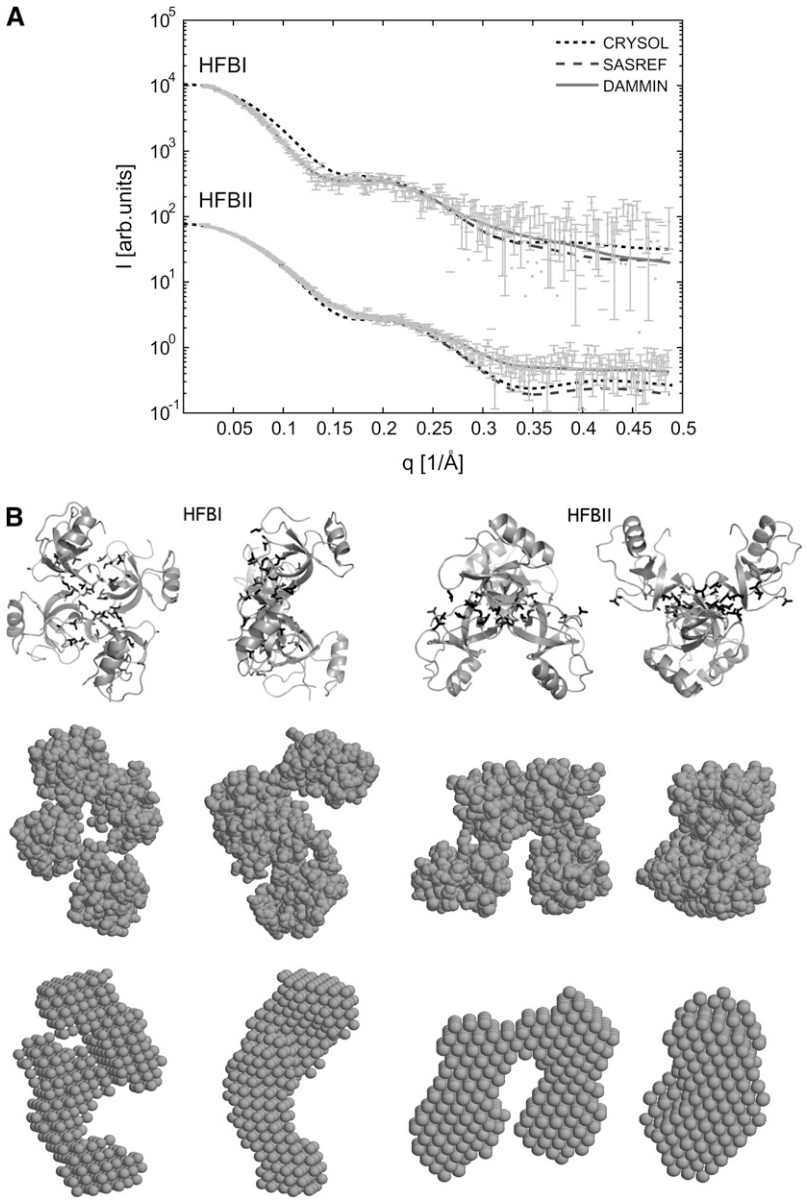

FIGURE 3 (*A*) Scattering intensity of HFBI at 1 mg/ml (*upper curve*) and HFBII at 2.5 mg/ml, with the scattering intensity of the single crystal tetramer computed by CRYSOL and experimental intensities fitted with SASREF and DAMMIN (see text for details). (*B*) The corresponding single crystal structures (*top row*), SASREF, and DAMMIN models. Columns 1 and 2 represent HFBI, columns 3 and 4 HFBII. The second (fourth) column is the first (third) turned by 90° over the vertical axis. In the single crystal structures, the black lines indicate the conserved aliphatic side chains in the hydrophobic patch (8,9).

Å; and that of the smallest ''tetramer'', consisting of two dimers from neighboring unit cells, is 20.7 Å. Thus the MM indicates that HFBII is dimeric at 0.5 mg/ml, whereas the Rg is closer to a crystal tetramer than to a dimer. However, the differences in the Rg are quite small, so the experimental Rg of 20.1 Å could also arise from an elongated dimer.

The distance distribution functions (see Fig. 4 for $c = 2.5$ mg/ml) were calculated from the scattering patterns of HFBII in all the concentrations. Because the intensity curves at the lowest concentrations have large statistical errors and there is possibly an equilibrium of different oligomers, the data at 2.5 mg/ml were used for modeling. Fig. 3 *A* shows the experimental intensity at 2.5 mg/ml, the scattering intensity of the tetramer in the crystal computed with CRYSOL, and intensities fitted with SASREF and DAMMIN. Fig. 3 *B* shows the corresponding models, which confirm that HFBII mainly forms tetramers in the present concentrations. The shape of the tetramer in solution and in the crystal is fairly similar. The only difference is that in the SASREF and DAMMIN models the tetramer is flat, whereas in the crystal the two dimers forming the tetramer are perpendicular to each other.

HFBI and HFBII in aqueous solution as a function of temperature

A change of temperature from 6.2°C to 60°C does not affect the association of HFBI at 2.5 mg/ml. The SAXS intensities below room temperature are all identical (data not shown). The intensity at the smallest angles decreases slightly as the temperature rises above 20°C, which is also seen as a small

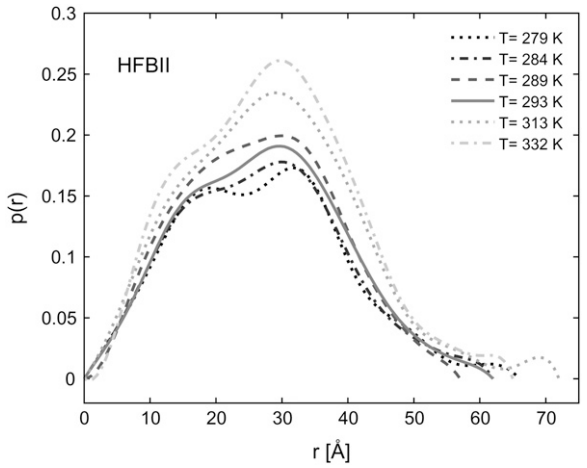

FIGURE 4 The distance distribution functions of HFBII at different temperatures.

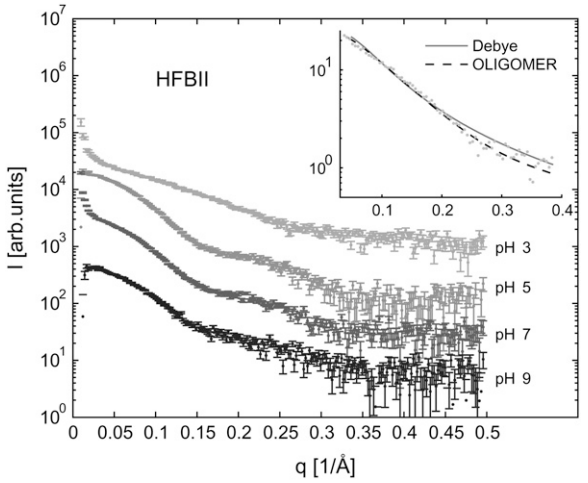

FIGURE 5 The scattering intensity of HFBII as a function of pH at pH values 3, 5, 7 (Hepes), and 9. The curves have been vertically lifted with respect to each other, all by a decade compared to the previous one. The inset shows the beginning of the scattering curve at pH 3. The experimental intensity has been fitted using a Debye coil model and by OLIGOMER.

decrease in Rg (Table 2). Either the structure becomes more compact or the interference effects between the oligomers become more important. In contrast to HFBI, the HFBII assemblies undergo gradual structural changes as a function of temperature. The positions of the individual monomers with respect to each other change, but the tetramer prevails. This is shown in the distance distribution functions of Fig. 4.

HFBI and HFBII in aqueous solution as a function of pH

All the measurements as a function of concentration and temperature, reported above, were conducted at a constant pH of 5. For HFBI, a change of pH from 3 to 6 does not change the structure, which means that the shapes presented in Fig. 3 prevail. Upon increasing the pH above 6, the Rg and $I(0)$ start to decrease. Otherwise the scattering patterns remain unchanged, which suggests that the decrease is due to the interference effects between the assemblies (data not shown). The isoelectric point of HFBI, determined by the program ProtParam (26), is $pI = 5.7$. Thus the increasing interference effects between the protein assemblies above pH 6 can be related to the change in the sign of the net surface charge.

HFBII has an isoelectric point of 6.7 (26) and behaves like HFBI under high pH conditions. At pH 9 the Rg, $I(0)$, and the maximum distance in the particle are smaller than at pH 5, indicating interference effects. The scattering curves at pH 6, 5, and 4 are almost identical. However, at the lowest pH value, 3, the tetrameric structure has clearly dissociated (Fig. 5). The scattering curve is fairly featureless, which could indicate (partial) unfolding of the protein. An unfolded protein can be described using a Debye coil model (27) with the Rg being a fitting parameter. In this case the best fit gives Rg = 18.5 Å. In Fig. 5 the intensity of this coil is compared to that of a model consisting of a mixture of coils, monomers, dimers, and tetramers. The parameters of the coils were fixed to the values obtained above, and the scattering intensities of the monomers, dimers, and tetramers are computed using CRYSOL. The volume fractions of these aggregates were fitted using the program OLIGOMER. This gives the volume fraction of unfolded coils as 0.829 ± 0.003 and monomers 0.171 ± 0.003. According to this model, there are no dimers or tetramers present in the solution. However, it should be noted that this approach cannot take into account the possible changes in the shapes of the protein assemblies from crystal to the solution, so the model should be treated with caution. Nevertheless, it is clear that the original assembly has broken down and at least partially unfolded. HFBII solution assemblies do not tolerate low pHs to the same extent as HFBI.

HFBI and HFBII in ethanol solutions

The role of the hydrophobic effect in the association of hydrophobins was studied by measuring HFBI and HFBII in 25%, 50%, and 65% ethanol solutions. Ethanol breaks the oligomers into monomers in a concentration-dependent manner. The dissociation is seen as a decrease in the Rg (Table 3). For HFBII, the Rg in 25% ethanol solution is already fairly close to the Rg of a monomer in the single crystal (Table 1), whereas for HFBI 50% ethanol solution is needed to break the original oligomers. Indeed, in 50% ethanol solution the scattering patterns of HFBI and HFBII resemble the scattering patterns of the corresponding single crystal monomers (Fig. 6). To further confirm the monomeric structure, the scattering intensities of HFBI and HFBII in 50% ethanol solution were fitted using the program GASBOR. The obtained models, also pictured in Fig. 6, show very compact monomers. Based on the Rg, in 65% ethanol both HFBI and HFBII also exist as monomers.

TABLE 3 The Rg as a function of ethanol concentration for HFBI and HFBII

	HFBI	HFBII
% EtOH	Rg (Å)	Rg (Å)
0	26.2 ± 0.4	21.3 ± 0.2
25	24.1 ± 1.0	13.4 ± 0.6
50	11.2 ± 0.5	10.5 ± 0.3
65	11.6 ± 0.4	11.3 ± 1.0

The error estimates for the Rg values are obtained from the differences between the GNOM values and the direct fit to the Guinier law.

To confirm that the changes in the Rg are not caused by the unfolding of the proteins, the stability of the native monomer structures of HFBI and HFBII in ethanol solutions were studied by observing secondary structures by circular dichroism (CD) (Supplementary Material). The CD spectra of HFBI and HFBII were very similar in 0%, 25%, 50%, and 65% ethanol solutions (Figure S1). Thus the native structures of HFBI and HFBII monomers are not changed in up to 65% ethanol. Also the addition of 2 mM DTT, which was used in the SAXS measurements to minimize radiation damage, did not alter the secondary structures of HFBI and HFBII according to the CD measurements (Supplementary Material). Therefore, the changes in Rg are not caused by protein denaturation but by changes in protein associations. The tetramers of HFBII break at lower ethanol concentrations than the more resistant tetramers of HFBI.

HFBI and HFBII in aqueous solution with different salts

HFBI and HFBII were measured in solutions with 0.5 M NaCl, $(NH_4)_2SO_4$, or $MnSO_4$ on the order of the Hofmeister series of salts (28,29). Indeed, the effects seen in the association of the proteins were in accordance with the Hofmeister series. The scattering curves of HFBI and HFBII in solution with sodium chloride were very close to the ones observed without a salt. With $(NH_4)_2SO_4$ and especially $MnSO_4$, a change from oligomers to larger assemblies is seen. Fig. 7 shows this gradual change for HFBI. The change looks very similar for HFBII (data not shown). On a double logarithmic scale (Fig. 7, *inset*) the solutions of HFBI and HFBII with $MnSO_4$ show power law behavior in low values of the scattering vector. Two regions with differing exponents can be distinguished. For HFBI, the first has an exponent −2.4 (fitting range 0.01–0.019 1/Å), and second −1.1 (fitting range 0.022–0.057 1/Å). For HFBII, the corresponding values are −1.5 (fitting range 0.01–0.022 1/Å) and −0.7 (fitting range 0.026–0.057 1/Å). Upon addition of salts along the Hofmeister series, the well-defined tetramers of HFBI and HFBII aggregate into larger assemblies. However, no signs of crystallization are detected.

DISCUSSION

HFBI and HFBII are two hydrophobin proteins from *T. reesei*. The amino acid sequence of HFBII is 69% similar to HFBI (15). The folded structures of HFBI and HFBII are similar (9,8), as are their previously studied hexagonal structures in thin films (19). However, in the association behavior in solution some differences between HFBI and HFBII could be seen. Both existed mainly as tetramers in solution, as seen also previously at 10 mg/ml (13), but now the assemblies of HFBI were shown to be more stable than those of HFBII. HFBI could tolerate changes in temperature and pH and addition of ethanol better than HFBII. In *T. reesei*, HFBI is found in the fungal cell walls (14), whereas

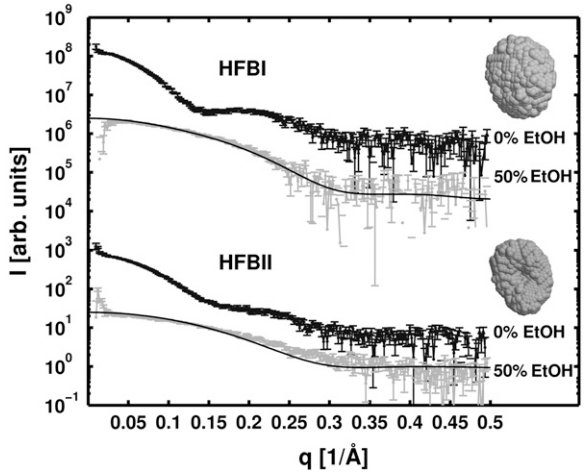

FIGURE 6 The SAXS intensities of HFBI and HFBII in 0% and 50% ethanol solution. The solid curves are the theoretical scattering curves of the HFBI and HFBII monomers computed with CRYSOL. The GASBOR models computed from the 50% ethanol solutions are also shown. The maximum distances of HFBI and HFBII in the GASBOR model are 30 and 32 Å, respectively.

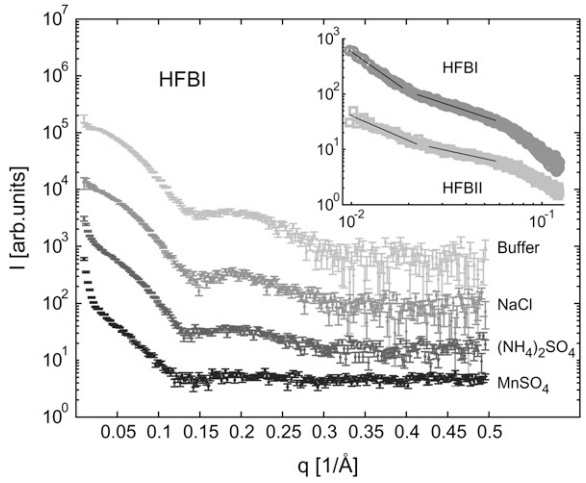

FIGURE 7 The scattering intensities of HFBI in buffer (*top*) and in solution containing 0.5 M NaCl, $(NH_4)_2SO_4$, and $MnSO_4$. (*Inset*) HFBI and HFBII in $MnSO_4$ (note the double logarithmic scale). The solid lines are the power laws fitted to the curves.

HFBII is secreted into the medium and is also found on the surface of the spores (15). The differences in the solution behavior of HFBI and HFBII could thus reflect their somewhat different functional roles in fungal life.

The quaternary structure of some proteins in their single crystal forms differ from that observed in the aqueous solution (e.g., 30). In the single crystal the asymmetric unit of HFBI is a tetramer (9). Its Rg (21.1 Å) and maximum distance in the particle (64 Å) are smaller than those determined here in solution. In solution the tetramer is slightly larger (Rg 25.1 Å) and more elongated, and monomers are not as tightly packed as in the crystal. For HFBII, the tetramer in solution is fairly similar to the tetramer in the single crystal. The single crystals of HFBI and HFBII were both grown from solutions containing salts: HFBII was crystallized from a 2 mM lithium sulfate, 10 mM $MnCl_2$ solution (8), whereas HFBI was crystallized from a 8 mg/ml solution with 0.1 M zinc sulfate in 0.1 M sodium cacodylate buffer at pH 6.5 (9). For HFBI a detergent was added to slow the crystallization. This might be attributable to the differences between the tetrameric assemblies in the single crystal and in the solution.

For both HFBI and HFBII the association in solution depends on the concentration. Here, using synchrotron radiation, we were able to conduct SAXS measurements in the concentration range 0.5–10 mg/ml. Based on the changes in the Rg and the MM, we concluded that the equilibrium of HFBII shifts from dimers to tetramers at around 1 mg/ml. Unfortunately, the assemblies at concentrations below 1 mg/ml could not be modeled due to large statistical errors in the data. Like HFBII, HFBI probably also forms dimers at low concentrations, but in the studied concentration range the tetramers dominate. The proportion of oligomers larger than tetramers increases with concentration. One way to find the possible structures of the larger oligomers is to start from the single crystals. The program PISA (31) lists all the potential assemblies in the crystal and analyzes their chemical stability in water. For HFBII the program gives the tetramer of Fig. 3 *B* as the most stable oligomer. For HFBI, it is an octamer. The detergents needed in the crystallization of HFBI were not found in the asymmetric unit (9) and thus were not included in the PISA calculation. The HFBI octamer is composed of four ''dimers'' from different asymmetric units, instead of two asymmetric unit tetramers. The Rg of the octamer is 34 Å. If the octamer was more stable than a tetramer in solution, then it should be the dominant oligomer, provided there is a suitable concentration. However, according to the SAXS results the tetramer stays the dominant oligomer. Furthermore, the scattering pattern of the PISA octamer does not resemble the experimental curves. Other octamers with scattering patterns closer to the experimental curves can be found in the crystal, for example, an octamer consisting of two (asymmetric unit) tetramers on top of each other. However, they are not classified as stable by PISA. This discrepancy could be due to the experimental conditions, such as the concentration or pH. However, it highlights the difficulty in predicting the solution assemblies based on the crystal structure.

The folded structures of both HFBI and HFBII contain a mainly hydrophilic surface with a hydrophobic patch. This amphiphilic structure explains the main features of the association behavior of HFBI and HFBII (12): the formation of oligomers in aqueous solution which allows the proteins to bury the hydrophobic surface areas and the dissociation of the oligomers upon addition of ethanol. Indeed, in the 50% ethanol solution HFBI and HFBII exist predominantly as monomers (Fig. 6, Table 3). Furthermore, addition of salts to the aqueous hydrophobin solution promotes the formation of larger assemblies. However, the details of the association behavior depend also on other interactions and factors, such as the shape of the monomers, which determine why the main oligomer in solution is a tetramer and not a dimer, for example.

The association behavior of HFBI and HFBII in solution is fairly similar to that of the class I hydrophobin SC3 (11). All the protein solutions contain an equilibrium of different oligomers. In contrast to HFBI and HFBII, the dominant oligomer in SC3 solution (50 mM sodium phosphate buffer at pH 7.0) was shown to be a dimer (11). Based on the hydrodynamic radius, the dimers were proposed to have an elongated shape. Low pH values did not affect the self-association of SC3, but at pH 9 the dominant oligomers were larger than tetramers. The self-association of SC3, like that of HFBI and HFBII, was proposed to be driven by hydrophobic interactions (11).

The relationship between the hydrophobin assemblies in solution and the self-assembled films on the air/water interface is unclear. Both are proposed to be due to the amphiphilic structure of the hydrophobin monomer (8), leading to surfactant-like behavior (12). In such a case one could expect the self-assembled film on the air/water interface to be a monolayer composed of monomers. However, Langmuir-Blodgett and Langmuir-Schaefer films of HFBI, imaged with atomic force microscopy, were observed to be crystalline and suggested to consist of oligomeric assemblies (17,18). Langmuir films of *T. reesei* hydrophobin HFBIII, studied with grazing-incidence x-ray diffraction, were composed of hexagonally ordered assemblies, in which part of the monomers were lifted with respect to each other (32). These examples indicate the presence of specific protein-protein interactions, which can also exist in solution. In such a case, one might also imagine that the self-assembled film consists of similar assemblies as there are in solution, with perhaps some changes in the quaternary structure.

The role of hydrophobins for fungal growth and physiology is still not well understood. They clearly have functions such as allowing the development of aerial structures and the formation of protective coatings on spores and fruiting bodies (33,34). Fungi have an important role in the ecosystem, for example in degradation of plant litter, and hydrophobins may play a central role in fungal colonization of the environment.

Hydrophobins are one way in which fungi adapt to their environment through adhesion and control of surface forces. Interactions of fungi with other organisms (either symbiotic or parasitic) are also very likely to be affected by hydrophobins. It has been suggested that hydrophobins cause hydrophobization of soil and may therefore have widespread environmental effects (35). The role of hydrophobins for environmental adaptation is supported by the early finding that hydrophobin genes are often very highly expressed (7). Here the hydrophobin tetramers were found to tolerate rather large changes in temperature and pH, which would facilitate their persistence in the soil. By studying the underlying structure-function relations in hydrophobins, better understanding of the ecological role of fungi can be obtained.

Our studies of hydrophobins so far have led to the conclusion that they act as surfactants but in a very different way than any other surfactants that have been described earlier (1). These differences give unique properties to hydrophobins (2,36). Molecular interactions and self-assembly are key components in understanding the origin of these unique properties. In this work we focused on these interactions, the shape and size of monomers and oligomers, and how they interact in solution under different conditions. The two *T. reesei* hydrophobins were found to form mainly tetramers in aqueous solutions, but the dynamic behavior of the tetramers revealed disparities possibly related to the different functional roles of the two proteins.

SUPPLEMENTARY MATERIAL

To view all of the supplemental files associated with this article, visit www.biophysj.org.

We acknowledge The European Molecular Biology Laboratory/Deutsches Elektronen–Synchtrotron for the provision of synchrotron radiation facilities and thank Dr. Manfred Roessle, Dr. Dmitri Svergun, and Teemu Ikonen for their assistance at the beamline X33.

The financial support from National Graduate School in Materials Physics (K.K.), Jenny and Antti Wihuri Foundation (K.K.), and National Graduate School in Informational and Structural Biology (G.R.Sz.) is gratefully acknowledged.

REFERENCES

1. Linder, M. B., G. R. Szilvay, T. Nakari-Setälä, and M. Penttilä. 2005. Hydrophobins: the protein-amphiphiles of filamentous fungi. *FEMS Microbiol. Rev.* 29:877–896.
2. Wösten, H. A. B., O. M. H. de Vries, and J. G. H. Wessels. 1993. Interfacial self-assembly of a fungal hydrophobin into a hydrophobic rodlet layer. *Plant Cell.* 5:1567–1574.
3. Wösten, H. A. B., F. H. J. Schuren, and J. G. H. Wessels. 1994. Interfacial self-assembly of a hydrophobin into an amphipathic protein membrane mediates fungal attachment to hydrophobic surfaces. *EMBO J.* 13:5848–5854.
4. van Wetter, M.-A., H. A. B. Wösten, J. H. Sietsma, and J. G. H. Wessels. 2000. Hydrophobin gene expression affects hyphal wall composition in *Schizophyllum commune*. *Fungal Genet. Biol.* 31:99–104.
5. Wösten, H. A. B., M.-A. van Wetter, L. G. Lugones, H. C. van der Mei, H. J. Busscher, and J. G. H. Wessels. 1999. How a fungus escapes the water to grow into the air. *Curr. Biol.* 9:85–88.
6. Wang, X., F. Shi, H. A. B. Wösten, H. Hektor, B. Poolman, and G. T. Robillard. 2005. The SC3 hydrophobin self-assembles into a membrane with distinct mass transfer properties. *Biophys. J.* 88:3434–3443.
7. Wessels, J. G. H. 1994. Developmental regulation of fungal cell wall formation. *Annu. Rev. Phytopathol.* 32:413–437.
8. Hakanpää, J., A. Paananen, S. Askolin, T. Nakari-Setälä, T. Parkkinen, M. Penttilä, M. B. Linder, and J. Rouvinen. 2004. Atomic resolution structure of the HFBII hydrophobin, a self-assembling amphiphile. *J. Biol. Chem.* 279:534–539.
9. Hakanpää, J., G. R. Szilvay, H. Kaljunen, M. Maksimainen, M. Linder, and J. Rouvinen. 2006. Two crystal structures of *Trichoderma reesei* hydrophobin HFBI—the structure of a protein amphiphile with and without detergent interaction. *Protein Sci.* 15:2129–2140.
10. Kwan, A. H. Y., R. D. Winefield, M. Sunde, J. M. Matthews, R. G. Haverkamp, M. D. Templeton, and J. P. Mackay. 2006. Structural basis for rodlet assembly in fungal hydrophobins. *Proc. Natl. Acad. Sci. USA.* 103:3621–3626.
11. Wang, X., J. F. Graveland-Bikker, C. G. de Kruif, and G. T. Robillard. 2004. Oligomerization of hydrophobin SC3 in solution: from soluble state to self-assembly. *Protein Sci.* 13:810–821.
12. Szilvay, G. R., T. Nakari-Setälä, and M. B. Linder. 2006. Behavior of *Trichoderma reesei* hydrophobins in solution: interactions, dynamics and multimer formation. *Biochemistry.* 45:8590–8598.
13. Torkkeli, M., R. Serimaa, O. Ikkala, and M. Linder. 2002. Aggregation and self-assembly of hydrophobins from *Trichoderma reesei*: low-resolution structural models. *Biophys. J.* 83:2240–2247.
14. Nakari-Setälä, T., N. Aro, N. Kalkkinen, E. Alatalo, and M. Penttilä. 1996. Genetic and biochemical characterization of the *Trichoderma reesei* hydrophobin HFBI. *Eur. J. Biochem.* 235:248–255.
15. Nakari-Setälä, T., N. Aro, M. Ilmén, G. Muñoz, N. Kalkkinen, and M. Penttilä. 1997. Differential expression of the vegetative and spore-bound hydrophobins of *Trichoderma reesei*: cloning and characterization of the *hfb2* gene. *Eur. J. Biochem.* 248:415–423.
16. Ritva, S., M. Torkkeli, A. Paananen, M. Linder, K. Kisko, M. Knaapila, O. Ikkala, E. Vuorimaa, H. Lemmetyinen, and O. Seeck. 2003. Self-assembled structures of hydrophobins HFBI and HFBII. *J. Appl. Cryst.* 36:499–502.
17. Paananen, A., E. Vuorimaa, M. Torkkeli, M. Penttilä, M. Kauranen, O. Ikkala, H. Lemmetyinen, R. Serimaa, and M. Linder. 2003. Structural hierarchy in molecular films of two class II hydrophobins. *Biochemistry.* 42:5253–5258.
18. Szilvay, G. R., A. Paananen, K. Laurikainen, E. Vuorimaa, H. Lemmetyinen, J. Peltonen, and M. B. Linder. 2007. Self-assembled hydrophobin protein films at the air/water interface: structural analysis and molecular engineering. *Biochemistry.* 46:2345–2354.
19. Kisko, K., M. Torkkeli, E. Vuorimaa, H. Lemmetyinen, O. H. Seeck, M. Linder, and R. Serimaa. 2005. Langmuir-Blodgett films of hydrophobins HFBI and HFBII. *Surf. Sci.* 584:35–40.
20. Svergun, D. I., and M. H. J. Koch. 2003. Small-angle scattering studies of biological macromolecules in solution. *Rep. Prog. Phys.* 66:1735–1782.
21. Tardieu, A., A. Le Verge, M. Malfois, F. Bonneté, S. Finet, M. Riès-Kautt, and L. Belloni. 1999. Proteins in solution: from x-ray scattering intensities to interaction potentials. *J. Cryst. Growth.* 196:193–203.
22. Zhang, F., M. W. A. Skoda, R. M. J. Jacobs, R. A. Martin, C. M. Martin, and F. Schreiber. 2007. Protein interactions studied by SAXS: effect of ionic strength and protein concentration for BSA in aqueous solutions. *J. Phys. Chem. B.* 111:251–259.
23. Konarev, P. V., M. V. Petoukhov, V. V. Volkov, and D. I. Svergun. 2006. ATSAS 2.1, a program package for small-angle scattering data analysis. *J. Appl. Cryst.* 39:277–286.

24. Verheul, M., J. S. Pedersen, S. P. F. M. Roefs, and K. G. de Kruif. 1999. Association behavior of native β-lactoglobulin. *Biopolymers.* 49:11–20.

25. Orthaber, D., A. Bergmann, and O. Glatter. 2000. SAXS experiments on absolute scale with Kratky systems using water as a secondary standard. *J. Appl. Cryst.* 33:218–225.

26. Gasteiger, E., C. Hoogland, A. Gattiger, S. Duvaud, M. R. Wilkins, R. D. Appel, and A. Bairoch. 2005. Protein identification and analysis tools on the ExPASy server. *In* The Proteomics Protocols Handbook. J. M. Walker, editor. Humana Press, Totowa, NJ. 571–607.

27. Kirste, R. G., and R. C. Oberthur. 1982. Synthetic polymers in solution. *In* Small-Angle X-Ray Scattering. O. Glatter and O. Kratky, editors. Academic Press, London. 387–432.

28. Kunz, W., J. Henle, and B. W. Ninham. 2004. 'Zur lehre von der wirkung der salze' (about the science of the effect of salt): Franz Hofmeister's historical papers. *Curr. Opin. Colloid Interface Sci.* 9:19–37.

29. Zhang, Y., and P. S. Cremer. 2006. Interactions between macromolecules and ions: the Hofmeister series. *Curr. Opin. Chem. Biol.* 10: 658–663.

30. Ferreira-da-Silva, F., P. J. B. Pereira, L. Gales, M. Roessle, D. I. Svergun, P. Moradas-Ferreira, and A. M. Damas. 2006. The crystal and solution structures of glyceraldehyde-3-phosphate dehydrogenase reveal different quaternary structures. *J. Biol. Chem.* 281:33433–33440.

31. Krissinel, E., and K. Henrick. 2005. Detection of protein assemblies in crystals. *In* CompLife. M. R. Berthold, R. C. Glen, K. Diederichs, O. Kohlbacher, and I. Fischer, editors. Springer-Verlag, Berlin, Heidelberg. 163–174.

32. Kisko, K., G. R. Szilvay, E. Vuorimaa, H. Lemmetyinen, M. B. Linder, M. Torkkeli, and R. Serimaa. 2007. Self-assembled films of hydrophobin protein HFBIII from *Trichoderma reesei*. *J. Appl. Cryst.* 40:355–360.

33. Talbot, N. J. 1999. Fungal biology. Coming up for air and sporulation. *Nature.* 398:295–296.

34. Kershaw, M. J., C. R. Thornton, G. E. Wakley, and N. J. Talbot. 2005. Four conserved intramolecular disulphide linkages are required for secretion and cell wall localization of a hydrophobin during fungal morphogenesis. *Mol. Microbiol.* 56:117–125.

35. Rillig, M. C., B. A. Caldwell, H. A. B. Wösten, and P. Sollins. 2007. Role of proteins in soil carbon and nitrogen storage: controls on persistence. *Biogeochemistry.* 85:25–44.

36. Cox, A. R., F. Cagnol, A. B. Russel, and M. J. Izzard. 2007. Surface properties of class II hydrophobins from *Trichoderma reesei* and influence on bubble stability. *Langmuir.* 23:7995–8002.